1848 *Biochemistry* **2011,** *50,* 1848–1856
DOI: 10.1021/bi101454f

BIOCHEMISTRY
including biophysical chemistry & molecular biology
Article

The Role of Local Hydration and Hydrogen-Bonding Dynamics in Ion and Solute Release from Ion-Coupled Secondary Transporters[†]

Chunfeng Zhao and Sergei Yu. Noskov*

Institute for Biocomplexity and Informatics and Department of Biological Sciences, University of Calgary, 2500 University Drive, BI558, Calgary, Alberta, Canada T2N 1N4

Received September 8, 2010; Revised Manuscript Received January 20, 2011

ABSTRACT: Recent progress in crystallographic studies of sodium-coupled secondary transporters has revealed striking similarities in the structural organization of ion and solute binding. Previous reports suggested that the Na2 sodium binding site in the neurotransmitter sodium symporter (NSS) leucine transporter (LeuT) is conserved across sodium/proton coupled secondary transporters of many distantly related families. This site is implicated in the conformational dynamics controlled by the binding and release of both translocated solute and ion(s) through a mechanism that largely remains unknown. In this study, we used extensive equilibrium molecular dynamics simulations, potential of mean force (PMF) computations, and quasi-harmonic analysis of the LeuT transporter with and without sodium ion bound at the Na2 site to delineate the role of this site in the conformational dynamics of the protein. PMF computations show that in presence of the sodium ion in Na2 the conserved T354 residue is locked into a single rotameric state in contrast to two degenerate states available in the absence of ion in Na2. Molecular dynamics (MD) simulations suggest the formation of a stable water wire from the cytoplasm to the Na2 site in the occluded state. It is plausible that local hydration plays an important role in transport cycle facilitating release of the ion from Na2. An unbinding of the ion from the Na2 site leads to a tightening of the extracellular thin gates and a destabilization of the intracellular thin gate and thus may promote an unbinding of the cotransported substrate. The study lends additional support to the hypothesis that one of the main drivers in the transport cycle of Na-coupled secondary transporters is the binding of the Na2 ion that controls dynamical equilibrium between an inward-facing to an outward-facing conformation.

Sodium-dependent secondary transporters represent a large family of proteins that harnesses the electrochemical gradient of sodium movement, driving an uphill translocation of their substrate molecules (*1*, *2*). There are many known families of sodium-coupled secondary transporters whose ligands span a broad range of substrates, such as amino acids, sugars, and biogenic amines, that are essential for cellular signaling, nutrition, and osmotic regulation (*3*−*6*). Despite their low sequence homology, recent structural studies have identified striking similarities in the topological organization of proteins from different families, such as the sodium-coupled leucine transporter LeuT[1] of the NSS family (*6*), the sodium−galactose symporter vSGLT of the SSS family (*4*), Mhp1 of the NCS1 family (*7*, *8*), BetP of the BCCTs family (*3*), and even two proton-coupled amino acid transporters, AdiC (*9*, *10*) and ApcT (*11*). These shared structural features (*1*, *2*, *12*) include a 2-fold symmetry with inverted repeats that involve 5 + 5 essential helices and a break in the TM helices that form the substrate and ion binding pocket (*12*). These structural similarities may suggest a general translocation mechanism.

The simplest and most appealing mechanism for ion-coupled substrate transport proposed to date is the alternating access mechanism (*1*, *2*, *13*). Briefly, the ion(s) and substrate bind to one face (extracellular) of the transporter, which then induces conformational changes, followed by translocation of the ion(s) and substrate to the opposite face (intracellular) of the membrane. The transporter then changes its conformation from inward-facing to outward-facing, thereby resetting the cycle. The ion/solute stoichiometry may vary depending on the transporter from 1Na:1S in vSGLT, to 2Na:1S in LeuT and BetP, and to 3Na:1S in the Glt_{Ph} aspartate transporter (*3*, *4*, *6*, *8*, *14*). Nevertheless, ion binding and dissociation provide a mechanistic force that drives this translocation cycle over and over. Structural studies on LeuT revealed the existence of at least one additional stable state for the transporter, the occluded state where ions and solute are bound to the transporter and both intracellular (IC) and extracellular (EC) gates are closed. For LeuT, this state has two Na^+ ions bound at sites Na1 and Na2 and the cotransported solute structurally couples to one of the sites (Na1). Surprisingly, it is the second solute-uncoupled sodium binding site (Na2) that is conserved among different transporters with known crystal structures of vSGLT (*4*) and Mhp1 (*7*, *8*). The structure of Na2 is shown in Figure 1. The binding and dissociation of the ion at the Na2 site may, therefore, provide a general mechanism for the

[†]This work was supported by the Discovery Grant from the National Sciences and Engineering Research Council of Canada (NSERC) to S. Yu.N. C.Z. is an Alberta Heritage Foundation for Medical Research Post-Doctoral Fellow, and S.Yu.N. is an Alberta Ingenuity New Faculty and AHFMR Scholar. The local computing resources were provided because of generous support from Canadian Foundation for Innovation Leaders Opportunity Award and AHFMR major equipment award to S.Yu.N.

*To whom correspondence should be addressed: tel, (403) 210 7971; fax, (403) 220 8655; e-mail, snoskov@ucalgary.ca.

[1]Abbreviations: MD, molecular dynamics; LeuT, leucine transporter; PDF, (atom−atom) pair distribution function; PMF, potential of mean force; TM, transmembrane; vSGLT, *Vibrio parahaemolyticus* sodium−galactose symporter.

 Published on Web 01/26/2011

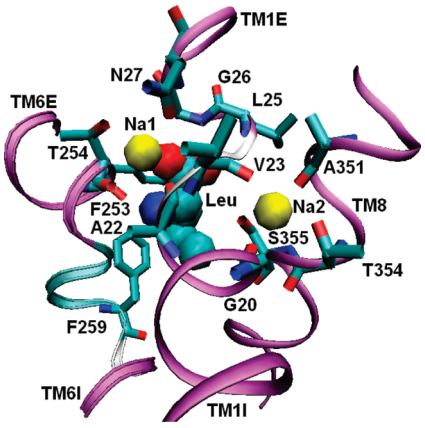

FIGURE 1: Structure of the LeuT Na2 site and its coupling to Na1 and the substrate binding site. The Na2 site is formed by residues from TM1 and TM8. The figure also shows the residues near the unwound regions of TM1 and TM6 that bind to the Na1 sodium and the leucine substrate. Na1 and Na2 sodium ions (yellow) and the leucine substrate are shown in ball representation. The transporter is shown in ribbon with helices in magenta and unwound regions in white or blue. Important residues from TMs 1, 6, and 8 that directly bind the ions and substrate are highlighted in stick representation.

conformational dynamics that lead to ion and substrate release into the cytoplasm. Although modulation of the transporter's conformational dynamics by binding and unbinding of Na^+ to Na2 is conceptually simple, the exact role of the ion that is structurally uncoupled from the cotransported substrate and the nature of the forces that lead to destabilization of the thermodynamically stable occluded state are still poorly understood (*1*). Previous studies suggest that the ion in the Na2 site may act as structure-stabilizing ion and may not be a part of the cooperative translocation mechanism at all (*15*). Other studies argued that the binding of the Na^+ ion to this site is required to enhance ion selectivity of this two-ion binding motif in LeuT and prevents binding of both K^+ and Li^+ (*16*, *17*). There are also reports showing that Na^+ binding is required for induction of the conformational changes that are essential in the translocation cycle (*12*, *18*). For example, recent review of thermodynamics of ion and solute binding to LeuT provided strong arguments on the fact that the dissociation of the two ions and the solute from LeuT is a cooperative event (*1*).

Experimental and simulation studies show that the sodium sites in the partially disassembled (ion-releasing state of the transporter) state of the vSGLT and Mhp1 transporters readily release Na^+ ion, forming the inward-facing state of the transporter (*7*, *19*, *20*). There are also suggestions that ion release leads to the destabilization of the thin IC gate, thereby inducing substrate dissociation from its corresponding binding site in the transporter into the bulk solution (*21*). At the same time, the Na2 site in the occluded state of the LeuT transporter is very stable through long simulations (100+ ns time scale) with or without the bound substrate (*22*, *23*). Obviously, the mechanisms that drive Na^+ release from a thermodynamically stable state where it is bound to a selective protein site remain unclear.

To elucidate the mechanism by which the sodium ion becomes dissociated from the transporter, we performed atomistic MD and free energy simulations on LeuT in explicit lipid bilayers with and without Na^+ bound to the Na2 site. While it is unlikely that ion dissociation and gating would occur simultaneously over 100 ns in our simulations of the thermodynamically stable state, differences in the hydration patterns, local side-chain rearrangement, and intrinsic protein dynamics provide insight into the structural mechanism for this dissociation and may clarify the order of events during the translocation of a substrate. In this study, our goal is to provide microscopic insight to investigate the conformational dynamics that occur at the Na2 site, which leads to the release of the ion and its consequences. Here, we present data on the ion-dependent hydration patterns around the Na2 binding pocket, the vibrational modes that were excited by Na^+ release, and local dynamics in hydrogen-bonding residues.

METHODS

Equilibrium Molecular Dynamics Simulations. The initial configuration of LeuT was taken from the X-ray coordinates that were reported by Yamashita et al. (*6*) (Protein Data Bank entry 2A65). The simulation system was built using a multistep membrane building procedure, which has been used in previous studies (*17*, *24*, *25*). The simulation box contained one transporter, sodium ions in the Na1 and Na2 sites, the leucine substrate, and 148 DPPC lipid molecules solvated by 100 mM NaCl in an aqueous solution. A snapshot of the full simulation box is shown in Figure S1 in the Supporting Information. MD simulations were carried out by CHARMM version c34b2 (*26*) and NAMD 2.6 (*27*, *28*) using the CHARMM27 force fields for proteins and lipids (*29*). The TIP3P model was used for the water molecules (*30*). The constant pressure/surface area/temperature (NPaT) ensemble was used for all simulations with pressure at 1 atm and temperature at 315 K. Long-range electrostatic interactions were calculated by the particle mesh Ewald (PME) algorithm with a 96 Å by 96 Å by 96 Å grid for a fast Fourier transform. Nonbonded interactions were switched off at 12−14 Å. Following a staged equilibration with a gradual decrease in harmonic constraints that act on heavy protein atoms, further equilibration was run for 5 ns without any configurational constraints. Next, the Na^+ ion was removed from the Na2 site to generate the Na2 free LeuT. Simulations with (denoted as the *Na1:Na2* system) and without (denoted as the *Na1:0* system) Na^+ bound to the Na2 site were monitored for more than 60 ns. The time step used for the simulations was 2 fs, and the coordinates of the MD trajectories were recorded every 5 ps.

Quasi-Harmonic Analysis. The principal modes of the internal dynamics of LeuT with and without the bound ion in Na2 were analyzed using the quasi-harmonic analysis option (QUASI) provided by the CHARMM program (*31*). For each system, the MD trajectories from NAMD were oriented and merged with the MERGE keyword in the DYNAMC module of CHARMM using the heavy atoms of the protein to eliminate the effect from translation and rotation of the protein. The principal component modes were then obtained with the QUASI key word in the VIBRAN module at a temperature of 315 K. Ten modes with lowest frequencies for each system were recorded for analysis.

PMF Computations for Torsional Surface. For each potential of mean force (PMF) calculation that described the rotation of the T354 side chain (dihedral $N-C_\alpha-C_\beta-O_\gamma$ of T354) with and without the bound Na^+ in Na2, 36 independent simulations at 200 ps (with a simulation time step of 1 fs) were carried out with a biasing harmonic potential centered on the dihedral angle, which was varied from 0° to 350° by a step of 10°, using a force constant of 100 kcal/(mol·rad^2). The biasing potential was applied using the MMFP option in the CHARMM program (*26*). Initial structures for the calculations were taken

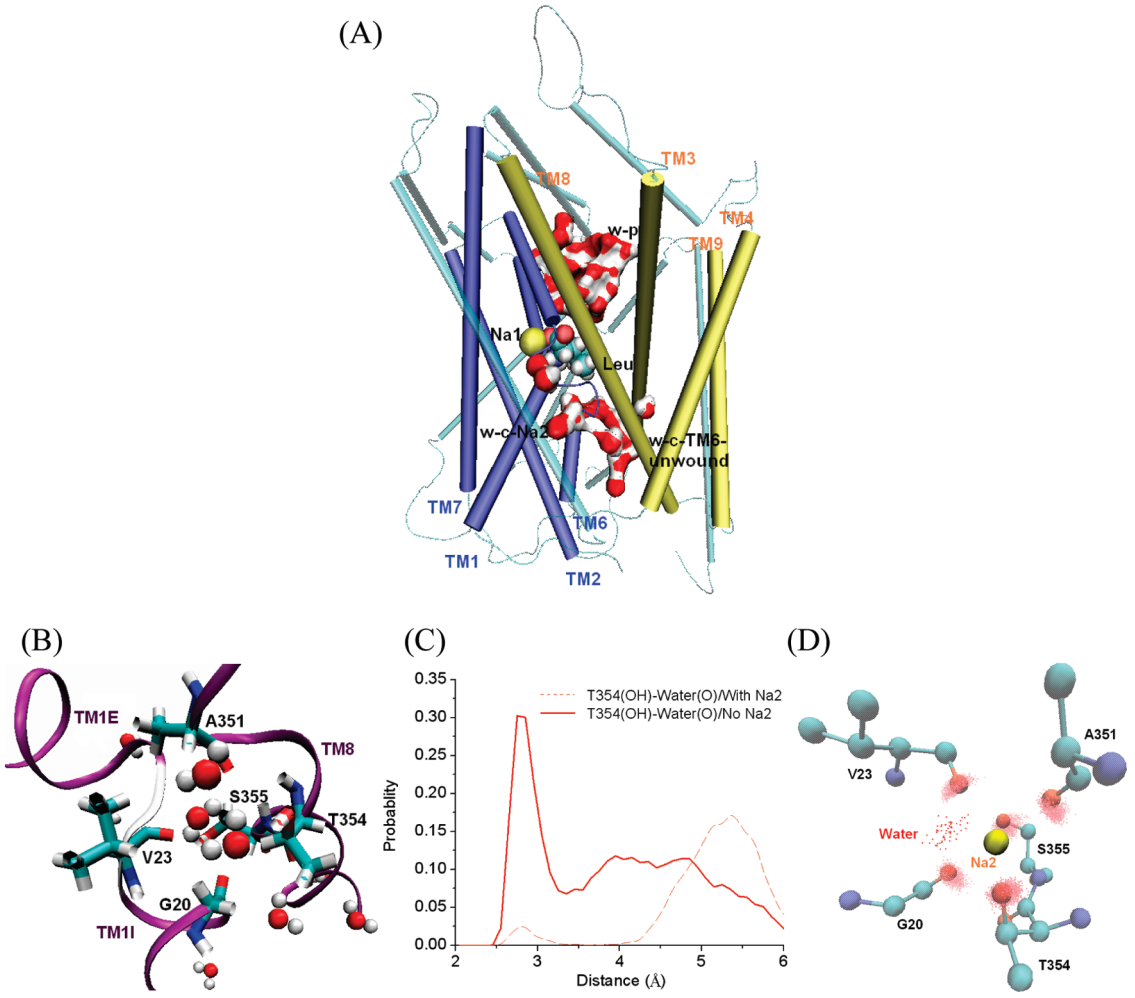

FIGURE 2: Local hydration of the substrate and ion binding sites. In (A), a snapshot from MD simulation of the LeuT with the Na2 Na^+ removed showing the two water wires (with water shown in surface representation) from cytoplasm leading to the empty Na2 binding site (w-c-Na2) and the unwound region of TM6 (w-c-TM6-unwound). The leucine substrate (ball, Leu) and bound Na^+ in Na1 (yellow ball, Na1) as well as water from periplasm (w-p) are also shown. The two water wires are mostly between the "bundle" (TMs 1, 2, 6, 7, in blue) and the "hash motif" (TMs 3, 4, 8, 9, in yellow). In (B), the Na2 sodium binding site of Na2 free LeuT is shown with water molecules nearby highlighted in a ball representation. In (C), the pair distribution functions of the distance between the hydroxyl oxygen of T354 and oxygen from nearby water molecules are shown for the Na2 bound (dashed) and Na2 free (solid) LeuT. In (D), an overlay of the Na2 binding site and the bound Na^+ for the frames obtained through equilibrium MD simulations of the occluded LeuT. Na^+ is shown as a yellow ball. The coordinating oxygens and water oxygens within 3 Å of the ion are shown in red dots. The coordinating residues are shown in ball and stick form for one frame to indicate the structure of the site.

from the equilibrium structures obtained in Equilibrium Molecular Dynamics Simulations. The weighted histogram analysis method (WHAM) (*32*−*34*) was then applied to obtain unbiased PMF.

RESULTS

Water Accessibility to Na2 Site and the Substrate Binding Site from Cytoplasm. Analysis of the equilibrium molecular dynamics trajectories suggests that water molecules can penetrate from cytoplasm into the protein core, where the ion and substrate binding sites locate. For the *Na1:0* system, two stable water wires from cytoplasm, with one to the Na2 site (w-c-Na2) and the other to the helix−break−helix region of TM6 of the substrate binding site (w-c-TM6-unwound), were rapidly formed within 5 ns of simulation. Figure 2A shows a snapshot of the transporter with water molecules that are within 15 Å of the substrate where these two water wires are evident.

The two water wires are mainly formed between the "bundle" (TMs 1, 2, 6, 7, shown in blue) and the "hash motif" (TMs 3, 4, 8, 9, shown in yellow). One major consequence of water penetration from cytoplasm is a steady increase in the local hydration of bound ions and a substrate. Interestingly, structural coupling between "rocking" of the bundle and the hash motif was proposed before. The reciprocal dynamics of these two structural elements is thought to be the major conformational driver in the transition from the occluded to inward-facing state of sodium-coupled transporters (*7*, *19*, *35*).

Notably, one of the coordinating groups of the Na2 site, the T354 hydroxyl oxygen, showed high probability of hydrogen bonding to water molecules accessed from cytoplasm. In Figure 2B, several water molecules stably reside around the vacant Na2 binding site. In Figure 2C, the pair (atom−atom) distribution functions (PDF) are shown for the hydroxyl oxygen of the T354 side chain and the oxygen of water molecules around for the whole course of equilibrium MD simulation. A PDF indicates the probability of finding the atom pair at a given distance. In the figure, the position of the first peak between heavy atoms at 2.8 Å corresponded to the oxygen−oxygen distance of a canonical hydrogen bond. The T354 side chain seems to play an essential role in the initial formation of the water

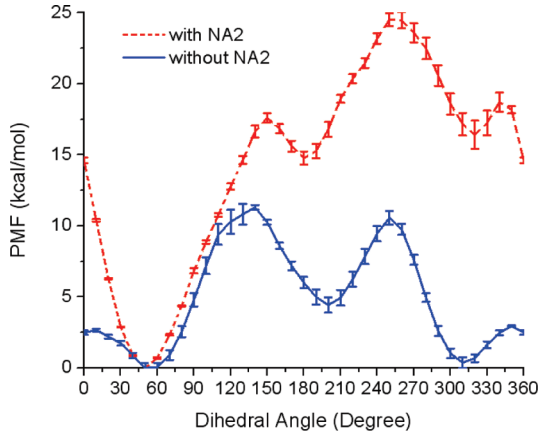

FIGURE 3: PMF for the reorientation of the N−C_α−C_β−O_γ of T354 of the Na2 binding site with (red) and without (blue) the bound Na^+. The PMF is plotted as a function of the dihedral angle. Error bars are the standard deviations of the computed free energy calculated by blocking the histograms to three blocks.

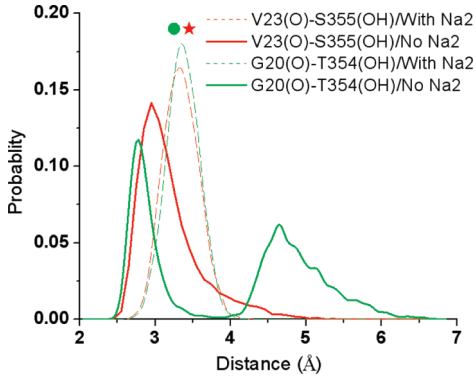

FIGURE 4: Pair distribution functions of oxygen−oxygen distance between V23(O)−S355(hydroxyl O) (red) and between G20-(O)−T354(hydroxyl O) (green) with and without the bound ion in Na2 are shown in dashed and solid lines, respectively. The experimental distances are marked in a red star and a green circle for V23(O)−S355(hydroxyl O) and G20(O)−T354(hydroxyl O) of the occluded LeuT with Na^+ bound in Na2, respectively.

wire. Once stable water is formed from the cytoplasm, an entire binding pocket with Na^+ at Na1 and bound solute become hydrated by the penetrating water molecules. In Supporting Information (Figure S2), similar PDF's show the increased hydration of critical residues forming binding pockets, including N27, F259, S355, and 1359, upon the removal of Na^+ in Na2.

In the *Na1:Na2* system where both Na^+ present, water molecules are still able to access the Na2 site from the cytoplasm. Although less frequently, the same water pathway (w-c-Na2) is noticed in our MD simulation for the *Na1:Na2* system. In Figure 2C, a similar PDF is shown for the fully occupied transporter (the dotted line). The probability of water penetration into the protein core has decreased substantially for *Na1:Na2* occupancy. Nevertheless, the peak that corresponds to direct hydrogen bonding between water and O_γ(T354) is still present at 2.8 Å. The conservation of this peak suggests that the formation of a hydrogen bond between T354 and a water molecule is still possible for the fully occupied occluded state of LeuT. The water molecules around the Na2 site can also occasionally directly bind to the ion in the Na2 site. Figure 2D plots an overlay of the Na2 site of the trajectory frames where water molecules within 3.0 Å (O−Na^+ distance) of Na^+ are shown. From Figure 2D, water molecules directly bind to Na^+ in Na2 roughly from the opposite face of the A351−G20/V23/S355/T354 pyramid. Figure S3 from Supporting Information shows PDF between the Na^+ in the Na2 site and water oxygen atoms. It has a well-defined peak around 2.5 Å, indicating formation of stable ion−water pairs. These depths of water penetration into the protein core of occluded LeuT were further illustrated by grand-canonical Monte Carlo (GCMC) simulations (for detailed methodology for GCMC, please see Method S1 in Supporting Information). In these GCMC simulations, a continuous water wire was stably formed for the occluded state of the transporter with both ions and substrate bound (data not shown), suggesting that wetting of these protein moieties is a thermodynamically favorable process.

Potential of Mean Force for the Rotation of T354 Side Chain. Equilibrium MD simulations were instrumental to highlight the role of T354 in the formation of water wire serving as an ion-controlled switch (Supporting Information Figure S4). To quantify the thermodynamic barriers for the rotation of the T354 side chain in LeuT for different ion occupancy, we calculated the potential of mean force (PMF) for the rotation of the dihedral N−C_α−C_β−O_γ for both *Na1:0* (solid blue line) and *Na1:Na2* (dashed red line) states (Figure 3). The *Na1:0* system displayed two major, and almost degenerate, minima at 310° and 50°. The free energy barrier separating these two minima was only about 2.5 kcal/mol. For the *Na1:Na2* system, the global minimum of the PMF was at 50°, which corresponded to the geometry reported in the crystal structure (*6*). The calculated barrier to the local minimum at 310° was about 17 kcal/mol, which may explain a very slow turnover rates observed for LeuT.

Interhelical Hydrogen Bonds Could Be Formed between TM1 and TM8 upon Removal of Na^+ in Na2. In LeuT the Na2 site (*6*) is formed by three backbone carbonyl oxygen atoms from G20 and V23 in the TM1 helix and A361 (TM8), and two side-chain hydroxyl oxygen atoms from T354 and S355 in the TM8 helix (Figure 1). In Figure 4, PDF's are shown for different oxygen pairs as a function of Na^+ presence in the site. In the Na^+ bound PDF's, the coordinating oxygen atoms displayed only minor displacements that corresponded to thermal fluctuations, indicated by the small width obtained in the principal PDF's of O(G20) to Oγ(T354) and O(V23) to Oγ(S355) that had a well-defined peak at ~3.3 Å, which is in agreement with the crystal structure (*6*). When the Na^+ is removed, functional groups forming the Na2 site showed considerable rearrangements. A new peak appeared at a distance of 4.7 Å in the PDF of O(G20) to Oγ(T354) (Figure 4), indicating that these two oxygen atoms became separated. A close examination of this rearrangement showed that rotation of the T354 side chain was the cause for this separation (Supporting Information Figure S4). Interestingly, the peaks at a closer distance (~2.8 Å for O(G20) to Oγ(T354) and ~3.0 Å for O(V23) to Oγ(S355)) indicate that interhelical hydrogen bonds could be formed between these residues upon the removal of Na^+ in Na2.

Increased Fluctuation of the Substrate and the Other Ion upon the Removal of Na^+ in Na2. As shown in Figure 1, the helix−break−helix region of TM1 plays an important role in the formation of binding sites for both sodium ions and the substrate (*1*, *6*). In addition to the residues (G20 and V23) that form the Na2 site, residues involved in Na1 sodium binding (A22(O) and N27(O_γ)) and in coordination of the leucine substrate (L25(N) and G26(N)) also originate from this helix−break−helix region, suggesting that the binding of ions and the substrate is coupled. We examined the distances between the

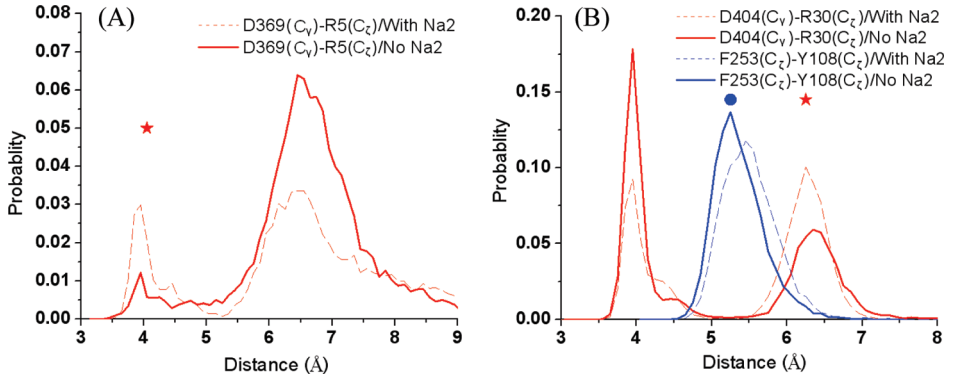

FIGURE 5: States of the proposed extracellular and intracellular gates with and without the bound ion in Na2. In (A), the pair distribution functions of D369(Cγ) and R5(Cζ) distance are plotted for Na2 bound (dashed) and Na2 free (solid) LeuT. The experimental distance is marked with a red star for D369(Cγ)−R5(Cζ) of the occluded LeuT with Na^+ bound in Na2. In (B), the pair distribution functions of D404(Cγ) and R30(Cζ) (red) as well as F253(Cζ) and Y108(Cζ) (blue) distances are plotted for Na2 bound (dashed) and Na2 free (solid) LeuT. The experimental distances are marked with a red star and a blue circle for D404(Cγ)−R30(Cζ) and F253(Cζ)−Y108(Cζ) of the occluded LeuT with Na^+ bound in Na2, respectively.

center of mass of LeuT and Na1 Na^+ and between centers of mass of LeuT and the leucine substrate with and without Na2 Na^+ bound. Removal of Na^+ in Na2 resulted in a modest increase in the fluctuations of the protein−ion (from 0.23 ± 0.02 to 0.26 ± 0.01 Å) and protein−solute (from 0.23 ± 0.01 to 0.27 ± 0.01 Å) distances.

Release of Na^+ from Na2 Promotes the Stochastic Tightening of the Extracellular Thin Gates and Opening of the Intracellular Thin Gate. An important effect of the dissociation of Na^+ from the Na2 site is the change in the dynamics of the proposed IC thin gate (*6*). This gate is formed by a salt bridge between R5 of TM1 and D369 of TM8 (*6*). In Figure 5A, the PDF for C_ζ of R5 and C_γ of D369 is shown. The presence of peaks around 4 Å indicates the formation of a direct salt bridge. These peaks are around the experimental distance of 4.1 Å (*6*). Direct comparison of this PDF between the *Na1:Na2* (dotted line) and *Na1:0* (solid line) states indicates a substantial decrease in the probability of salt-bridge formation after ion removal from Na2. Nevertheless, even in the *Na1:Na2* system, the IC thin gate R5−D369 could be open. Our MD simulations also showed that the proposed EC thin gates (*6*), F253−Y108 and D404-R30, appear to be tightened with the removal of the Na^+ from the Na2 site, indicated by the more pronounced peaks at the closer distances in Figure 5B. Analysis of the simulation trajectory showed that an opening of the D404−R30 EC thin gate is primarily governed by dynamics of TM10, consistent with the reported conformational gating proposed for another transporter (Mhp1) (*7*).

Quasi-Harmonic Analysis of the Principal Modes of Intrinsic Transporter Motions in the Helix−Break−Helix Regions and the Intracellular Thin Gate. Normal mode analysis of the protein dynamics is known to provide important insights on the low-frequency dynamics that governs intrinsic conformational changes in the protein (*36*). The low-frequency principal modes were evaluated from quasi-harmonic analysis of MD trajectories. The results show more substantial impact of ion occupancy on a low-frequency dynamics of the LeuT transporter. In Figure 6A,B, the principal modes of LeuT that dictate the intrinsic movement of the helix−break−helix regions of TM1 and TM6 are shown for the *Na1:0* and *Na1:Na2* states of LeuT. The removal of Na^+ from Na2 leads to a noticeable increase in the flexibility and amplitudes of movements in the helix−break−helix regions, especially that of TM6 (Figure 6(A)), compared to that in the fully loaded state (Figure 6B). Figure 6C shows the second mode of the *Na1:0* state of LeuT, in which the oscillation of the TM1 tail, corresponding to the stochastic opening/closures of the IC thin gate, can be observed.

DISCUSSION

Local Hydration of Ion and Substrate Binding Sites from Cytoplasm Seems to Be a General Feature in Many Sodium-Coupled Secondary Transporters. While there has been no report of the existence of the water pathways from cytoplasm to ion and substrate binding sites in LeuT under equilibrium states, the crystal structure of LeuT (*6*, *37*) suggests the presence of water molecules around the Na2 sodium binding site. Our results of water accessibility in the LeuT Na2 binding site are consistent with previous reports that demonstrated a permeation pathway from cytoplasm in the human serotonin transporter (analogue of LeuT) by Forrest et al. (*35*). Solvent accessibility data from the Na^+/proline transporter PutP (*38*) (belongs to the sodium/solute symporter family and a homologue of vSGLT) demonstrated that two amino acid residues, S340 and T341 (corresponding to T354 and S355 of LeuT), show solvent accessibility. Recent study of vSGLT (*19*) also indicated that water molecules had accessed the sodium-binding site from the cytoplasm, leading to substrate and/or ion release. Similar results for water accessibility were also recently reported for the sodium-binding site in Mhp1 (*7*). While our manuscript was in review, another theoretical study (*39*) reported on a possibility of a water access pathway formation for the inward-facing model of LeuT. Combined together, evidence from experiment and theory alike suggests that the mechanism that leads to water accessibility from the cytoplasm into the Na2 site may be a general feature in many sodium-coupled secondary transporters. Therefore, the access of water molecules from the cytoplasm to the Na2 site is likely the first step in the destabilization of the occluded form of the transporter, and binding/unbinding of an ion serves as a conformational switch.

Na^+ Releasing from the Na2 Site Might Be Facilitated by Side-Chain Rotation of T354, Local Hydration, and Interhelical Hydrogen Bond Formation. Oxygen−oxygen PDF's of the fully loaded occluded LeuT (Figure 4) show that the Na2 sodium binding site holds up during the course of equilibrium MD simulation, indicated by the narrow oxygen−oxygen distance distributions around their experimental

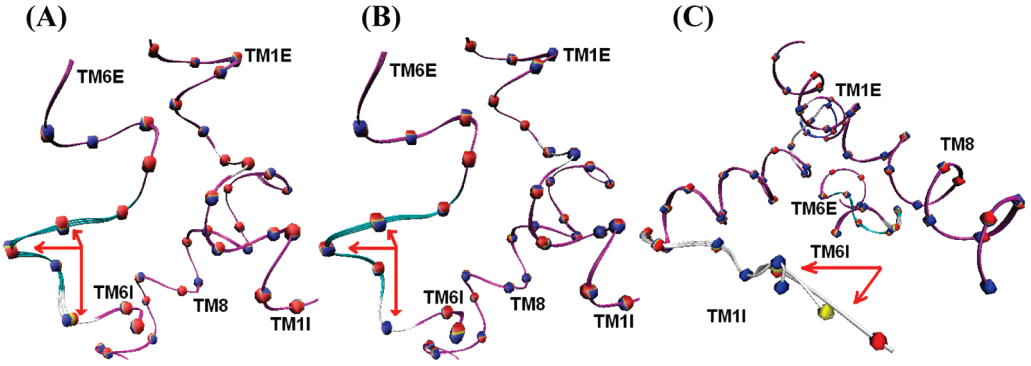

FIGURE 6: In (A), the fourth principal component mode (PC4) that features the motion of the ions and substrate binding region of TMs 1, 6, and 8 for Na2 free LeuT is shown. In (B) the same principal component mode (PC4) is shown for Na2 bound LeuT. Please note that comparing to the Na2 free LeuT in (A), less motion is indicated in the helix−break−helix region of TM6. In (C), the second principal component mode (PC2) of Na2 free LeuT highlighting the motion of the D369−R5 intracellular thin gate in shown.

values (*6*). By contrast, when the Na^+ is removed, we noticed the possibility of disruption of the Na2 site, evident by the peak appearing at a distance of 4.7 Å in the PDF of O(G20) to Oγ (T354) (Figure 4). We noticed the T354 side chain was the cause for this disruption (Supporting Information Figure S4). Specifically, when the dihedral N−C_α−C_β−O_γ of T354 changes from one local minimum of ~50° to the other local minimum of ~310° (Figure 3 blue line), the distance between O(G20) and Oγ (T354) changes roughly from 2.8 to 4.7 Å (Figure 4 solid green line). These data indicate that the side chain of T354 might be the "weak" group of the Na2 site and it might serve as a "latch" that could be loosened to release Na^+ from the site. This proposal is partially supported by recent reported inward-releasing (vSGLT (*2*, *19*)) and inward-facing (Mhp1 (*7*)) crystal structures, which all showed the disassembly of the conserved sodium binding site by the rotation of TM8, part of the so-called "hash motif", away from TM1, part of the so-called "bundle". Upon the potential open or loosening of the latch, water molecules around T354 and the Na2 site would readily hydrate the sodium ion and facilitate its inward release (*19*). In LeuT, rotation of T354 combined with an increase of hydration around the Na2 site results in reduced energetic penalty for Na^+ dissociation from the site and may set up a series of events leading to conformational transition with rocking of the "hash motif" relative to the "bundle". Figure 2C shows that even for the fully loaded *Na1:Na2* state (dotted line), water molecules can form favored interaction with the T354 side chain, which will compensate the free energy loss due to the lost interaction between T354 O_γ and Na^+ upon Na^+ releasing. The importance of local hydration in the dynamics of coordinating ligands has been illustrated in many studies of K channels (*40*). Another driving force for the destabilization of Na^+ in the Na2 site might be interhelical hydrogen bonding between the carbonyl oxygen atom of V23 and the hydroxyl group of the S355 side chain. Formation of this intraprotein hydrogen bond could result in the removal of the coordinating functional groups from the Na^+ coordination shell. In a recent study on vSGLT, it was shown that a interhelical hydrogen bond between S365 (corresponding to S355 in Leut) and E68, a residue in the helix−break−helix region of TM1 and (correspondingly) close to V23 in LeuT, plays an important role in stabilizing the inward-facing structure of vSGLT (*7*, *19*, *35*).

The proposed mechanism of ion removal from Na2 shares some striking similarities with the C-type inactivation mechanism in potassium channels. The rapid C-type inactivation in potassium channels is thought to be controlled by carbonyl flipping in the selectivity filter and the formation of new hydrogen bonds, thereby switching the channels from a conductive to a nonconductive conformation (*41*). Notably, the flipping occurs for very polar groups, such as carbonyl groups, even in presence of an ion in the binding site. This simple mechanism provides a molecular level support to conformational dynamics proposed before for Mhp1, vSGLT, and HT5 (*7*, *19*, *35*). As shown in Figure 2D, although the probability is low (~1% indicated by the peak from 2.05 to 2.95 in Supporting Information Figure S3), Na^+ in Na2 can bind to a water oxygen atom directly. In summary, thermodynamic stabilization from water molecules binding to Na^+ and hydrogen bonding to T354 may help to offset the destabilized interaction between Na^+ and the Na2 site. The formation of an interhelical hydrogen bond between V23 and S355 may also partially compensate for free energy loss from releasing Na^+ from the Na2 site to drive translocation. To get a qualitative estimate of binding affinity for Na^+ to Na2, we performed free energy simulations of the ion uncharging. The resulting free energy corresponds to the electrostatic component of equilibrium binding free energy to a given state of the transporter. The computations suggest that ΔG_{elec} for Na^+ in Na2 is around −6.2 kcal/mol from the FEP computation (Supporting Information Methods S2). The micromolar range of binding combined with possible free energy compensations discussed above suggests that the releasing of Na^+ from its binding pocket is thermodynamically possible.

Removal of the Coupled Na^+ in Na2 and Increased Local Hydration Destabilize the Substrate and the Na^+ in Na1. The crystal structure of LeuT and many previous studies have shown that the ion and substrate binding are coupled. Release of the Na2 ion may affect the binding of both the Na1 ion and the substrate to facilitate their subsequent release and thus is a cooperative event. The removal of Na2 ion affects stability of Na1 leading to widening of the probability distribution for ion−N27 distance (Supporting Information Figure S5). A recent experimental investigation suggests that its homologue (N101) in HT5 transporters plays a critical role in ion-dependent conformational dynamics (*42*). Other than the intrinsic coupling (sharing coordinating residues from same regions) between ions and the substrate, one other potential reason for the increased rattle of the Na1 ion and the substrate is the increased local hydration of the helix−break−helix regions of TM1 and TM6 by water molecules accessed from cytoplasm through the two pathways illustrated in Figure 2A. For example, there was a notable increase in protein−water interactions between the backbone and

side-chain atoms of F259 in the *Na1:0* state of the LeuT compared to the *Na1:Na2* state of the transporter (Supporting Information Figure S2B). Similar results were obtained for S355 and I359 residues (Supporting Information Figure S2C,D). These residues are known to be essential in the formation of the high-affinity and high-specificity hydrophobic pocket that accommodates the nonpolar side chain of the leucine substrate (*6*). The interaction between N27 of TM1 and water molecules also increased slightly (Supporting Information Figure S2A), which may affect the binding of the substrate and the Na1 ion. Release of the substrate will likely lead to a release of the Na1 ion from its binding pocket. Previous free energy simulations performed on LeuT demonstrated that the presence of carboxylate functional groups from the substrate was essential for the high-affinity binding of Na^+ to Na1 (*25*). Therefore, removal of Na^+ from the Na2 site would lead to destabilization of the substrate and the Na1 ion binding pockets. The effect of this destabilization on the protein dynamics can be illustrated with the principal component analysis (PCA) of the vibrational modes in Figure 6A,B, where the removal of Na^+ from Na2 leads to a considerable increase in the flexibility of the TM6 helix−break−helix region (Figure 6A) compared to that in the fully loaded *Na1:Na2* state (Figure 6B).

Removal of Na^+ from Na2 Might Favor the Transformation of LeuT from Outward-Facing to Inward-Facing Conformation (42). As shown in the Release of Na^+ from Na2 Promotes the Stochastic Tightening of the Extracellular Thin Gates and Opening of the Intracellular Thin Gate and Quasi-Harmonic Analysis of the Principal Modes of Intrinsic Transporter Motions in the Helix−Break−Helix Regions and the Intracellular Thin Gate sections, the release of Na^+ from Na2 reinforces the EC thin gates but promotes an opening of the IC thin gate. The tightening of the D404−R30 EC thin gate is achieved mostly by ion-induced movement of D404, which belongs to TM10. Interestingly, TM10 forms the proposed extracellular thin gate of Mhp1 (*7*). One should note, however, that in Mhp1 the proposed thin gates are formed by an entire helix (TM5 for IC thin gate and TM10 for EC thick gate) (*7*). MD simulations combined with PCA analysis suggest that ion-coupled opening of the R5−D369 thin gate is mainly achieved by the movement of TM1I. This is consistent with the change in ion and substrate releasing of the vSGLT, where TM1I flexes by about 13° at the kink in the helix−break−helix region (*19*). Therefore, a still growing line of evidence lends support to the idea that the transition from outward-facing conformations to inward-facing conformations is associated with the relative movement of the "hash motif" to the "bundle" (*7*, *19*, *35*). Our simulations show that penetrating water molecules destabilize the Na2 site, leading to a release of the Na^+ ion. As a result an entire cleft between TM1I and TM8 gets hydrated. PCA analysis of different ion loads of LeuT discussed above allows us to speculate that in absence of Na^+ in Na2 further hydration of the "hash motif" and "bundle" subdomains promotes low-frequency movements that correspond to "rocking" of the "hash motif" relative to the "bundle" subdomain. This simple mechanism shows how hydration and ion binding/unbinding to Na2 may facilitate an outward-facing to inward-facing transformation of LeuT.

The idea of ion-controlled conformational dynamics in secondary transporters is further supported by the recent EPR study of LeuT by Claxton et al., which showed that the binding of Na^+ increases accessibility of the extracellular vestibule and induces an outward-facing conformation (*21*). The ion binding is also thought to trigger opening of the extracellular gate in an unrelated sodium-coupled transporter Glt_{Ph}, where subsequent binding of a substrate is thought to be closing it (*43*). Nevertheless, even with the Na^+ present at Na2, there is a finite probability of the IC thin gate R5−D369 being open as shown by Figure 5A, in good accord with independent computational interrogation of LeuT dynamics (*39*) and structural studies of Mhp1 transporter.(*7*) Thus, an opening and closing of the thin gates is a stochastic process. The equilibrium distribution between open and closed states and probability of shifting from one state to another depend on several factors such as hydration of the pocket and presence/absence of an ion in the binding site in close analogy to multistate models of ion channel and voltage-dependent probabilities of gated states, that dates back to pioneering work of Hodgkin and Huxley (*44*) and its extension by Sakmann and Neher (*45*).

Potential Implications to the Alternating Access Mechanism. Despite the wide range of substrates transported by several families of ion-coupled secondary transporters, the conservation of the LeuT Na2 ion-binding site indicates some general cotransporting mechanisms. We demonstrated that, starting from an outward-facing occluded state, solvent access from cytoplasm may help to release the ion in Na2, dissemble the site, and encourage rapid hydration of the protein core, which in turn may facilitate the transformation of the transporter from outward-facing occluded to inward-facing conformation. With the translocation of the substrate (and other ions), the transporter would be in the inward-facing open state when the "hash motif" is relatively rotated away from the "bundle". To reset the stage, the binding of Na^+ to Na2 would drive the transporter to change its conformation from inward-facing open to outward-facing open (*21*). The locking-in of polar hydroxyl groups of the T/S-rich 350−355 motif of TM8 ensures ion stabilization and corresponding destabilization of the extracellular gate in the transporter. With the binding of a substrate (and other ions) and subsequent conformational changes, the transporter comes back to the outward-facing occluded state (*7*, *21*). This proposed mechanism complies with the structures and ion/substrate bound states of current known crystal structures (Supporting Information Figure S6).

Many secondary transporters display reversibility of transport (*46*). The mechanism proposed here provides some glimpses of how such a reversibility of transport can be achieved. A plausible explanation is that the inward-facing releasing state and the inward-facing open state (Supporting Information Figure S6) are separated by small free energy barriers (*12*). In this situation, a substrate might bind to the inward-facing open conformer of the transporter from cytoplasm. The binding of the substrate helps to facilitate the formation of the Na2 binding site (and partially affects hydration patterns of entire pocket) and encourages the binding of sodium ion from cytoplasm. The substrate binding pocket displays considerable hydrophobicity, and thus partial dehydration might be a thermodynamically favorable process. The transporter might further change its conformation to outward-facing occluded, and the substrate and ion could be released to periplasm subsequently to complete the reverse transport. Here, a similar assumption is made that the binding/releasing of substrate to periplasm might be a low free energy barrier process and could be facilitated by favorable (for reverse transport) substrate concentration gradient.

CONCLUSIONS

A combination of molecular dynamics, free energy, and quasi-harmonic computations has revealed general principles that underlie the conformational changes that may be controlled by the release of an ion from the conserved Na2 site in LeuT. These studies revealed that water accessibility is possible in the Na2 site from the intracellular side for both *Na1:Na2* and *Na1:0* structures of the occluded state. The formation of a water wire from cytoplasm to Na2 site may facilitate ion release and lead to the rearrangement of the interhelical network. Our findings are in agreement with the crystal structure of the inward-facing vSGLT (*19*) and Mhp1 (*7*) structures and physiological studies carried out on the SERT (HT5) transporter (*35*). The interaction between water and T354 may help to open the Na2 binding site. We also found that an interhelical hydrogen bond between S355 and V23 was formed upon the removal of Na2 ion, which may play an important role in the release of the ion. Our simulations also indicate that the removal of Na^+ in Na2 encourages rapid local hydration of the protein core between the "bundle" and "hash motif" subdomains, increases the fluctuation of the Na^+ in Na1 and the substrate, tightens the extracellular thin gates of F253−Y108 and D404−R30, and increases the probability of opening the intracellular thin gate of LeuT formed by R5 and D369.

ACKNOWLEDGMENT

The discussions with Drs. E. Wright, J. Abrahmson, E. Gouaux, H. Weinstein, L. Shi, H. S. Mchaourab, and J. E. Cuervo are gratefully acknowledged. The authors are also indebted to the anonymous reviewers whose comments aided greatly discussion on the mechanism of transport. The computing resources of WestGrid, Canada, and the IBM Blue Gene machines provided by BlueFern, University of Canterbury New Zealand, are also acknowledged.

SUPPORTING INFORMATION AVAILABLE

Methods for GCMC simulation and FEP computation and six figures. This material is available free of charge via the Internet at http://pubs.acs.org.

REFERENCES

1. Krishnamurthy, H., Piscitelli, C. L., and Gouaux, E. (2009) Unlocking the molecular secrets of sodium-coupled transporters. *Nature 459*, 347–355.
2. Abramson, J., and Wright, E. M. (2009) Structure and function of Na^+-symporters with inverted repeats. *Curr. Opin. Struct. Biol. 19*, 425–432.
3. Ressl, S., van Scheltinga, A. C. T., Vonrhein, C., Ott, V., and Ziegler, C. (2009) Molecular basis of transport and regulation in the Na^+/betaine symporter BetP. *Nature 458*, 47–U41.
4. Faham, S., Watanabe, A., Besserer, G. M., Cascio, D., Specht, A., Hirayama, B. A., Wright, E. M., and Abramson, J. (2008) The crystal structure of a sodium galactose transporter reveals mechanistic insights into Na^+/sugar symport. *Science 321*, 810–814.
5. Rudnick, G. (2006) Serotonin transporters—Structure and function. *J. Membr. Biol. 213*, 101–110.
6. Yamashita, A., Singh, S. K., Kawate, T., Jin, Y., and Gouaux, E. (2005) Crystal structure of a bacterial homologue of Na^+/Cl-dependent neurotransmitter transporters. *Nature 437*, 215–223.
7. Shimamura, T., Weyand, S., Beckstein, O., Rutherford, N. G., Hadden, J. M., Sharples, D., Sansom, M. S. P., Iwata, S., Henderson, P. J. F., and Cameron, A. D. (2010) Molecular basis of alternating access membrane transport by the sodium-hydantoin transporter Mhp1. *Science 328*, 470–473.
8. Weyand, S., Shimamura, T., Yajima, S., Suzuki, S., Mirza, O., Krusong, K., Carpenter, E. P., Rutherford, N. G., Hadden, J. M., O'Reilly, J., Ma, P., Saidijam, M., Patching, S. G., Hope, R. J., Norbertczak, H. T., Roach, P. C. J., Iwata, S., Henderson, P. J. F., and Cameron, A. D. (2008) Structure and molecular mechanism of a nucleobase-cation-symport-1 family transporter. *Science 322*, 709–713.
9. Gao, X., Lu, F. R., Zhou, L. J., Dang, S. Y., Sun, L. F., Li, X. C., Wang, J. W., and Shi, Y. G. (2009) Structure and mechanism of an amino acid antiporter. *Science 324*, 1565–1568.
10. Fang, Y. L., Jayaram, H., Shane, T., Kolmakova-Partensky, L., Wu, F., Williams, C., Xiong, Y., and Miller, C. (2009) Structure of a prokaryotic virtual proton pump at 3.2 angstrom resolution. *Nature 460*, 1040–1043.
11. Shaffer, P. L., Goehring, A., Shankaranarayanan, A., and Gouaux, E. (2009) Structure and mechanism of a Na^+-independent amino acid transporter. *Science 325*, 1010–1014.
12. Forrest, L. R., Kramer, R., and Ziegler, C. (2011) The structural basis of secondary active transport mechanisms. *Biochim. Biophys. Acta 1807*, 167–188.
13. Jardetzk, O. (1966) Simple allosteric model for membrane pumps. *Nature 211*, 969.
14. Yernool, D., Boudker, O., Jin, Y., and Gouaux, E. (2004) Structure of a glutamate transporter homologue from *Pyrococcus horikoshii*. *Nature 431*, 811–818.
15. Celik, L., Schiott, B., and Tajkhorshid, E. (2008) Substrate binding and formation of an occluded state in the leucine transporter. *Biophys. J. 94*, 1600–1612.
16. Noskov, S. Y., and Roux, B. (2008) Control of ion selectivity in LeuT: Two Na^+ binding sites with two different mechanisms. *J. Mol. Biol. 377*, 804–818.
17. Caplan, D. A., Subbotina, J. O., and Noskov, S. Y. (2008) Molecular mechanism of ion-ion and ion-substrate coupling in the Na^+-dependent leucine transporter LeuT. *Biophys. J. 95*, 4613–4621.
18. Zhao, C. F., Lei, S., and Noskov, S. Y. (2010) unpublished results.
19. Watanabe, A., Choe, S., Chaptal, V., Rosenberg, J. M., Wright, E. M., Grabe, M., and Abramson, J. (2010) The mechanism of sodium and substrate release from the binding pocket of vSGLT. *Nature 468*, 988–U162.
20. Li, J., and Tajkhorshid, E. (2009) Ion-releasing state of a secondary membrane transporter. *Biophys. J. 97*, L29–L31.
21. Claxton, D. P., Quick, M., Shi, L., de Carvalho, F. D., Weinstein, H., Javitch, J. A., and Mchaourab, H. S. (2010) Ion/substrate-dependent conformational dynamics of a bacterial homolog of neurotransmitter: Sodium symporters. *Nat. Struct. Mol. Biol. 17*, 822–U868.
22. Shi, L. (2010) personal communication.
23. Shi, L., Quick, M., Zhao, Y. F., Weinstein, H., and Javitch, J. A. (2008) The mechanism of a neurotransmitter: Sodium symporter—Inward release of Na^+ and substrate is triggered by substrate in a second binding site. *Mol. Cell 30*, 667–677.
24. Zhao, C. F., Caplan, D. A., and Noskov, S. Y. (2010) Evaluations of the absolute and relative free energies for antidepressant binding to the amino acid membrane transporter leut with free energy simulations. *J. Chem. Theory Comput. 6*, 1900–1914.
25. Noskov, S. Y. (2008) Molecular mechanism of substrate specificity in the bacterial neutral amino acid transporter LeuT. *Proteins: Struct., Funct., Bioinf. 73*, 851–863.
26. Brooks, B. R., Bruccoleri, R. E., Olafson, D. J., States, D. J., Swaminathan, S., and Karplus, M. (1983) CHARMM: A program for macromolecular energy, minimization, and dynamics calculations. *J. Comput. Chem. 4*, 187–217.
27. Phillips, J. C., Braun, R., Wang, W., Gumbart, J., Tajkhorshid, E., Villa, E., Chipot, C., Skeel, R. D., Kale, L., and Schulten, K. (2005) Scalable molecular dynamics with NAMD. *J. Comput. Chem. 26*, 1781–1802.
28. Kumar, S., Huang, C., Zheng, G., Bohm, E., Bhatele, A., Phillips, J. C., Yu, H., and Kale, L. V. (2008) Scalable molecular dynamics with NAMD on the IBM Blue Gene/L system. *IBM J. Res. Dev. 52*, 177–188.
29. MacKerell, A. D., Bashford, D., Bellott, M., Dunbrack, R. L., Evanseck, J. D., Field, M. J., Fischer, S., Gao, J., Guo, H., Ha, S., Joseph-McCarthy, D., Kuchnir, L., Kuczera, K., Lau, F. T. K., Mattos, C., Michnick, S., Ngo, T., Nguyen, D. T., Prodhom, B., Reiher, W. E., Roux, B., Schlenkrich, M., Smith, J. C., Stote, R., Straub, J., Watanabe, M., Wiorkiewicz-Kuczera, J., Yin, D., and Karplus, M. (1998) All-atom empirical potential for molecular modeling and dynamics studies of proteins. *J. Phys. Chem. B 102*, 3586–3616.
30. Jorgensen, W. L., Chandrasekhar, J., Madura, J. D., Impey, R. W., and Klein, M. L. (1983) Comparison of simple potential functions for simulating liquid water. *J. Chem. Phys. 79*, 926–935.

31. Brooks, B. R., Brooks, C. L., Mackerell, A. D., Nilsson, L., Petrella, R. J., Roux, B., Won, Y., Archontis, G., Bartels, C., Boresch, S., Caflisch, A., Caves, L., Cui, Q., Dinner, A. R., Feig, M., Fischer, S., Gao, J., Hodoscek, M., Im, W., Kuczera, K., Lazaridis, T., Ma, J., Ovchinnikov, V., Paci, E., Pastor, R. W., Post, C. B., Pu, J. Z., Schaefer, M., Tidor, B., Venable, R. M., Woodcock, H. L., Wu, X., Yang, W., York, D. M., and Karplus, M. (2009) CHARMM: The biomolecular simulation program. *J. Comput. Chem. 30*, 1545–1614.
32. Allen, T. W., Andersen, O. S., and Roux, B. (2006) Molecular dynamics—Potential of mean force calculations as a tool for understanding ion permeation and selectivity in narrow channels. *Biophys. Chem. 124*, 251–267.
33. Roux, B. (1995) The calculation of the potential of mean force using computer simulations. *Comput. Phys. Commun. 91*, 275–282.
34. Kumar, S., Bouzida, D., Swendsen, R. H., Kollman, P. A., and Rosenberg, J. M. (1992) The weighted histogram analysis method for free-energy calculations on biomolecules. 1. The method. *J. Comput. Chem. 13*, 1011–1021.
35. Forrest, L. R., Zhang, Y. W., Jacobs, M. T., Gesmonde, J., Xie, L., Honig, B. H., and Rudnick, G. (2008) Mechanism for alternating access in neurotransmitter transporters. *Proc. Natl. Acad. Sci. U.S.A. 105*, 10338–10343.
36. Bahar, I., Lezon, T. R., Bakan, A., and Shrivastava, I. H. (2010) Normal mode analysis of biomolecular structures: Functional mechanisms of membrane proteins. *Chem. Rev. 110*, 1463–1497.
37. Singh, S. K., Piscitelli, C. L., Yamashita, A., and Gouaux, E. (2008) A competitive inhibitor traps LeuT in an open-to-out conformation. *Science 322*, 1655–1661.
38. Hilger, D., Bohm, M., Hackmann, A., and Jung, H. (2008) Role of Ser-340 and Thr-341 in transmembrane domain IX of the Na^+/proline transporter PutP of *Escherichia coli* in ligand binding and transport. *J. Biol. Chem. 283*, 4921–4929.
39. Shaikh, S. A., and Tajkhorshid, E. (2010) Modeling and dynamics of the inward-facing state of a Na^+/Cl^- dependent neurotransmitter transporter homologue. *PLoS Comput. Biol. 6*, e1000905.
40. Noskov, S. Y., and Roux, B. (2007) Importance of hydration and dynamics on the selectivity of the KcsA and NaK channels. *J. Gen. Physiol. 129*, 135–143.
41. Berneche, S., and Roux, B. I. (2005) A gate in the selectivity filter of potassium channels. *Structure 13*, 591–600.
42. Henry, L., Iwamoto, H., Field, J. R., Kaufmann, K., Dawson, E. S., Jacobs, M. T., Adams, C., Felts, B., Zdravkovic, I., Armstrong, V., Combs, S., Rudnick, G., Noskov, S. Y., DeFelice, L., Meiler, J., and Blakely, R. D. (2011) A conserved asparagine residue in TM1 of the serotonin transporter dictates chloride-coupled neurotransmitter transport, *Nat. Struct. Mol. Biol.* (submitted for publication).
43. Focke, P., Moenne-Loccoz, P., and Larsson, H. P. (2011) Opposite movement of the external gate of a glutamate transporter homologue upon binding co-transported sodium compared to substrate, *J. Neurosci.* (in press).
44. Hodgkin, A. L., and Huxley, A. F. (1952) A quantitative description of membrane current and its application to conduction and excitation in nerve. *J. Physiol.* (*London*) *117*, 500–544.
45. Neher, E., and Sakmann, B. (1992) The patch clamp technique. *Sci. Am. 266*, 44–51.
46. Poolman, B., and Konings, W. N. (1993) Secondary solute transport in bacteria. *Biochim. Biophys. Acta 1183*, 5–39.